Matrix-dependent adhesion of vascular and valvular endothelial cells in microfluidic channels†‡

Edmond W. K. Young,[ab] Aaron R. Wheeler*[bc] and Craig A. Simmons*[ab]

Received 14th August 2007, Accepted 31st August 2007
First published as an Advance Article on the web 14th September 2007
DOI: 10.1039/b712486d

The interactions between endothelial cells and the underlying extracellular matrix regulate adhesion and cellular responses to microenvironmental stimuli, including flow-induced shear stress. In this study, we investigated the adhesion properties of primary porcine aortic endothelial cells (PAECs) and valve endothelial cells (PAVECs) in a microfluidic network. Taking advantage of the parallel arrangement of the microchannels, we compared adhesion of PAECs and PAVECs to fibronectin and type I collagen, two prominent extracellular matrix proteins, over a broad range of concentrations. Cell spreading was measured morphologically, based on cytoplasmic staining with a vital dye, while adhesion strength was characterized by the number of cells attached after application of shear stresses of 11, 110, and 220 dyn cm^{-2}. Results showed that PAVECs were more well spread on fibronectin than on type I collagen ($P < 0.0001$), particularly for coating concentrations of 100, 200, and 500 μg mL^{-1}. PAVECs also withstood shear significantly better on fibronectin than on collagen for 500 μg mL^{-1}. PAECs were more well spread on collagen compared to PAVECs ($P < 0.0001$), but did not have significantly better adhesion strength. These results demonstrate that cell adhesion is both cell-type and matrix dependent. Furthermore, they reveal important phenotypic differences between vascular and valvular endothelium, with implications for endothelial mechanobiology and the design of microdevices and engineered tissues.

Introduction

All blood-contacting surfaces in the body are lined by a single layer of endothelial cells. These cells play a critical role in maintaining normal function of blood vessels,[1] heart valves,[2] and other cardiovascular tissues. Endothelial cells reside on a basement membrane comprised of a mixture of extracellular matrix (ECM) proteins, including varying amounts of fibronectin, vitronectin, type I and type IV collagen, and laminin.[3] Endothelial cells adhere to the basement membrane *via* integrins, a family of transmembrane heterodimeric glycoproteins that physically link the ECM, the cell surface, and the intracellular cytoskeleton.[4,5] The ECM not only provides a substrate for cell adhesion, but also actively regulates cell processes, such as proliferation, migration, and differentiation through integrin-mediated signaling.[5] Integrins also are responsible in part for transducing mechanical signals generated by blood flow-induced shear stress on the luminal surface of the endothelium.[6] Notably, endothelial response to shear stress is strongly ECM- and integrin-dependent.[7] Further, endothelial cells from different anatomic sites—for example those from the heart valves *versus* those from the blood vessels—respond uniquely to shear stress.[8] Thus, understanding endothelial cell signaling and mechanotransduction mechanisms relies heavily on elucidating the role of specific cell–matrix interactions.

The majority of endothelial cell shear studies have been conducted using "macroscale" setups, such as parallel plate flow chambers,[9,10] cone-and-plate devices,[11] and co-culture systems,[12] mainly because cell culture techniques at this scale are well established, and information on the design of these systems is well documented. Increasingly, microscale technologies are being used to create endothelial constructs and study endothelial cell biology. Microchannel devices have been fabricated to culture endothelial cells within confined geometries,[13,14] in biodegradable elastomeric networks,[15] on gelatin-based substrates (with epithelial cells),[16] on surface micropatterns,[17] in co-culture with other cell types,[18] and on modular collagen gels for the vascularization of engineered tissues.[19] The utility of endothelial microdevices and endothelialized constructs for cell biology and tissue engineering applications[19,20] depends on adequate cell adhesion and elicitation of appropriate cell responses to microenvironmental cues.

In this study, we investigated endothelial cell adhesion to substrates coated with fibronectin and type I collagen (two important ECM proteins), over a range of six coating concentrations. We further investigated differences between two similar, but distinct cell populations: primary endothelial

[a]*Department of Mechanical & Industrial Engineering, University of Toronto, 5 King's College Road, Toronto, Ontario, Canada, M5S 3G8. E-mail: simmons@mie.utoronto.ca; Fax: +1-416-978-7753; Tel: +1-416-946-0548*
[b]*Institute of Biomaterials & Biomedical Engineering, University of Toronto, 164 College Street, Toronto, Ontario, Canada, M5S 3G9. E-mail: awheeler@chem.utoronto.ca; Fax: +1-416-946-3865; Tel: +1-416-946-3864*
[c]*Department of Chemistry, University of Toronto, 80 St. George St., Toronto, Ontario, Canada, M5S 3H6*
† The HTML version of this article has been enhanced with colour images.
‡ Electronic supplementary information (ESI) available: Theory and complementary experiments. See DOI: 10.1039/b712486d

cells from the aorta *versus* those from the aortic heart valve. These experiments, representing 24 experimental conditions, would have been formidable using macroscale shear stress setups. The use of a parallel microfluidic network of test channels, however, facilitated the experimental design because it permitted the parallel analysis of multiple conditions rather than the serial analyses that would be required when using conventional methods. Furthermore, the system provided the usual microscale benefits of low reagent consumption and well characterized flow behavior. With this approach, we discovered significant differences in the ability of the two cell types to spread and adhere on different proteins. These novel observations contribute to a greater understanding of endothelial cell biology, particularly at the microscale, and identify cell type-specific behaviors with implications for the design of microdevices and engineered tissues.

Materials and methods

Device design and fabrication

The microchannel pattern of the shear devices used in this study was similar to the multisample device design by Lu *et al.*[21] In our design, eight identical parallel microchannels of 516 μm width and 59 μm depth were connected to a single inlet reservoir *via* a symmetric branching network (Fig. 1). The branches were designed to ensure the same hydrodynamic resistance through all eight fluidic paths.

The microfluidic shear devices were formed from PDMS and glass using the rapid prototyping technique.[22] Briefly, channel patterns were drawn in AutoCAD and printed at high resolution on a transparent photomask. Masters were fabricated by spin-coating SU-8-25 negative photoresist (Microchem, Newton, MA, USA) on glass slides that had been cleaned in piranha solution (70% sulfuric acid, 30% hydrogen peroxide, 30 min). After pre-baking, exposure, and post-exposure baking, the photoresist layer was developed by gentle agitation in SU-8 developer (Microchem). After development, masters were examined by profilometry (WYKO) at nine different random locations, and the feature depth was found to be 58.5 $\pm$ 4.2 μm, thus confirming feature height uniformity. Poly(dimethylsiloxane) (PDMS) (Sylgard 184, Dow Corning, Midland, MI, USA) in a 10 : 1 ratio of base to curing agent was poured over the masters, exposed to vacuum to remove air bubbles, and cured at 70 °C for at least four hours. A piranha-washed glass slide and a PDMS cast of the microchannel pattern were both rinsed in isopropyl alcohol (IPA), plasma treated for 90 s (Harrick Plasma, Ithaca, NY, USA), and then assembled with polyethylene tubing as inlet ports for eventual microfluidic injection and withdrawal.

Cell culture

Unless otherwise stated, all chemicals and reagents for cell isolation and culture were purchased from Sigma–Aldrich Canada; fluorescent dyes were from Molecular Probes

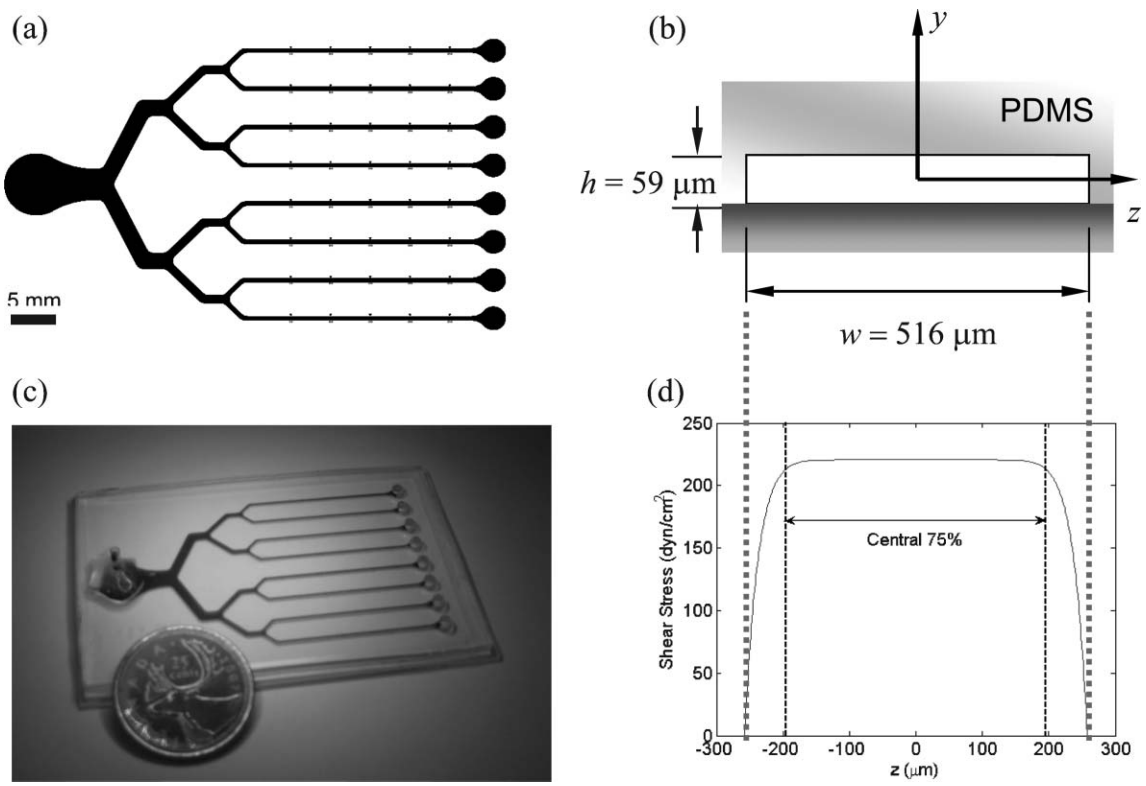

Fig. 1 (a) Parallel microfluidic shear device pattern, consisting of eight microchannels of 516 μm width. Scale bar = 5 mm. (b) Cross section of one microchannel with width w = 516 μm and height h = 59 μm. (c) Photograph of assembled PDMS–glass microfluidic shear device. (d) Shear stress distribution on channel midplane (y = 0) from side wall to side wall (-258 μm $\leqslant z \leqslant$ 258 μm). The central 75% is exposed to approximately constant shear stress (less than 5% difference from shear stress at z = 0).

(Carlsbad, CA, USA), and all other materials were purchased from Fisher Scientific Canada.

Aortic heart valves were dissected from fresh pig hearts obtained at a local abattoir (Quality Meat Packers, Toronto, Canada). Primary porcine aortic valve endothelial cells (PAVECs) were isolated from the valve leaflets within four hours of death by enzymatic digestion in a solution of 60 U mL^{-1} collagenase and 2.0 U mL^{-1} dispase for 2.5 h at 37 °C, followed by scraping to dislodge the cells. Isolated cells were cultured for three to four days in EGM-2 basal medium with SingleQuots (Cambrex Clonetics) supplemented with 20% fetal bovine serum (FBS) and 1% penicillin–streptomycin (P–S). A pure endothelial cell population was obtained from these first-generation cells using a MACS magnetic cell sorting system (Miltenyi Biotec, Auburn, CA, USA) according to the manufacturer's instructions and based on expression of CD31, an endothelial cell marker not expressed in valve fibroblasts. Purified endothelial cells were subsequently expanded in M199 supplemented with 10% FBS and 1% P–S in flasks pre-coated with 3% (w/v) gelatin, and frozen for later use. PAVECs between passages 4 and 7 were used in all reported experiments.

As a model of vascular endothelial cells, we used primary porcine aortic endothelial cells (PAECs) generously donated by Lowell Langille (University of Toronto). The aorta is the major blood vessel leaving the heart, just downstream from the aortic heart valve. Cells were thawed and expanded in M199 supplemented with 5% FBS, 5% calf serum (CS), and 1% P–S. All reported experiments used PAECs between passages 4 and 7.

Experimental preparation

Three hours prior to experimentation, cells (PAVECs or PAECs) were labeled with vital nuclear and cytoplasmic fluorescent dyes to aid in their visualization. Cells were incubated with Hoechst 33342 nuclear dye (2 μg mL^{-1} in supplemented M199 medium appropriate to the cell type) for 30 min at 37 °C and 5% CO_2, and then with CellTracker Green cytoplasmic dye (5 μM in serum-free M199 medium) for an additional 30 min at 37 °C and 5% CO_2. Finally, cells were maintained in fresh supplemented M199 medium until experimentation.

Prior to protein loading, the microchannels were sterilized by rinsing with 70% ethanol (10 min), followed by phosphate buffered saline (PBS) (10 min). PBS was then pushed out of the microchannels by flushing with sterile air from the inlet port. Two proteins were used in this study, human plasma fibronectin (FN) (Invitrogen—Gibco, Carlsbad, CA, USA) and rat-tail type I collagen (Col-I) (Becton Dickinson, Mississauga, ON, Canada). FN was diluted to desired concentration with supplemented medium (appropriate for cell type), while Col-I was diluted with sterile 0.02 N acetic acid. Five solutions of each protein were prepared: 500, 200, 100, 50, and 10 μg mL^{-1}. To coat the microchannels with proteins, 15 μL of each solution were added to the outlet reservoir of a microchannel on the device (*i.e.*, reservoirs on the right side of Fig. 1a). The remaining reservoirs were filled with various controls, *i.e.*, 0 μg mL^{-1} protein. After loading, suction was applied from the inlet port to draw the protein solutions from each reservoir into their respective microchannels. To prevent mixing of protein solutions, suction was ceased before the interface of the solutions reached any branch in the network. Thus, it was important to clear the microchannels with sterile air before coating to track this process. Compared to previous methods of coating microchannels with proteins,[21] this method resulted in considerable reduction in solution use, representing a concrete example of the often-cited advantage of low reagent consumption on microscale platforms.

After the proteins were drawn into the microchannels, the device was incubated at room temperature for 30 min to allow sufficient protein adsorption onto the underlying glass surface. After rinsing with ~1 mL of supplemented medium, bovine serum albumin (BSA, 1% w/v in PBS) was flushed through the network and incubated (30 min, 37 °C) to block non-specific cell adhesion. Microchannels were rinsed and maintained in supplemented medium until analysis.

Cell spreading and adhesion strength assays

Cells labeled with Hoechst and CellTracker Green vital dyes were trypsinized from the flasks and suspended at 10 million cells mL^{-1}. Using a syringe, the concentrated cell suspension was injected into the protein-coated microchannel network where the cells dispersed uniformly (Fig. 2). The device was incubated at 37 °C with 5% CO_2 for two hours to allow initial cell attachment and spreading on the channel surfaces. Observations were made immediately after the two hour incubation using an inverted fluorescent microscope (Leica), and fluorescent images were taken with a CCD camera (Hamamatsu). Cell areas were quantified using the ImageJ software package (NIH) to trace cell cytoplasmic borders.

To investigate adhesion strength, attached cells were subjected to increasing levels of flow-induced shear stress over a 12 min period. Culture medium was dispensed using a syringe pump (Harvard Apparatus series 11, Harvard, Holliston, MA, USA) at 12 mL h^{-1} for the first 4 min, 120 mL h^{-1} for the next 4 min, and 240 mL h^{-1} for the final 4 min. These flow rates translated to shear stresses of 11, 110, and 220 dyn cm^{-2}, respectively, based on the Purday approximation,[23]

$$\tau_w = \frac{2\mu Q}{wh^2}\left(\frac{m+1}{m}\right)(n+1) \quad (1)$$

where τ_w is the wall shear stress, Q is the volumetric flow rate, m and n are empirical constants related to channel aspect ratio

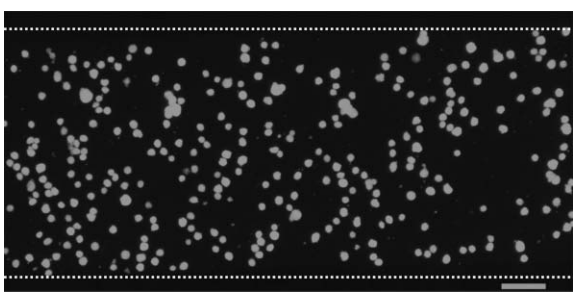

Fig. 2 PAECs after initial injection into microchannels at 10 million cells mL^{-1}. Cells were rounded, uniformly dispersed, and labeled with brightly fluorescing CellTracker Green cytoplasmic dye. White dotted lines indicate side walls of microchannel. Scale bar = 100 μm.

(see ESI‡), width w = 516 μm, height h = 59 μm, and viscosity of the culture medium at 37 °C is $\mu = 0.72 \times 10^{-3}$ kg m^{-1} s^{-1}, as measured with a Cannon–Fenske capillary viscometer. Note that eqn (1) is similar in form to the parallel plate approximation of $\tau_w = 6\mu Q/wh^2$. Fluorescent images were taken after each 4 min shear period, at three separate locations, x = 10, 15, and 20 mm from the start of each straight 30 mm long microchannel section. Cell counting (based on nuclear staining) was performed using ImageJ, and cell counts from the three locations were averaged to give a mean cell count for each microchannel.

Two control experiments were also performed to examine how quickly cells detached over time, and to evaluate whether initial low shear stress levels preconditioned cells for detachment at higher shear stresses in the approach outlined above. The first experiment comprised repeating the standard shear assay of 11, 110, and 220 dyn cm^{-2} at 4 min intervals and capturing images every 30 s over the 12 min period to obtain intermediate timepoints. The second experiment comprised applying 220 dyn cm^{-2} for 12 min, also with images captured every 30 s. Results are presented for experiments performed with PAVECs on 50 μg mL^{-1} FN. Similar results were observed with other combinations of cell type, protein type, and coating concentration.

To facilitate statistical analyses of acquired data, we created an adhesion strength parameter (ASP), ϕ, defined as

$$\phi = \frac{1}{3}(F_1 + F_2 + F_3) \quad (2)$$

where F_1, F_2, and F_3 are the normalized fractions of remaining cells at t = 4, 8, and 12 min, respectively. ASP averages the percentage of remaining cells over the course of the shear assay, and therefore, accounts for adhesion strength at all three nominal shear stress levels. Each adhesion strength time profile can thus be represented by a single metric measuring the propensity for a given cell type to remain adhered to a specific protein.

Flow characterization

To confirm that flow rates were uniformly distributed throughout the network, particle streak velocimetry[24] was used to measure velocities in each microchannel. Briefly, 1 μm fluorescent microspheres (FluoSpheres F8819, Molecular Probes) diluted in ethanol were pumped through microchannels at prescribed flow rates using a syringe pump. As illustrated in Fig. 3, images of particle streaklines were focused on the midplane between the top and bottom channel surfaces and captured using a CCD camera mated to an inverted fluorescent microscope (Olympus IX-71). The length of the longest streakline in each image was measured, and the average of these lengths determined the maximum velocity, u_{max}, for a given channel. We found measured maximum velocities to be consistent with theoretical predictions from the Purday approximation.[23] Furthermore, variability between channels within the same network was less than 10%. We note that ~12% of the channel width along each of the side walls was predicted to be lower than 95% of the shear stress found in the rest of the channel (see Fig. 1d). Therefore, only cells in the central 75% of the microchannels were counted during analysis of cell adhesion. A detailed description of our flow characterization is provided in the ESI.‡

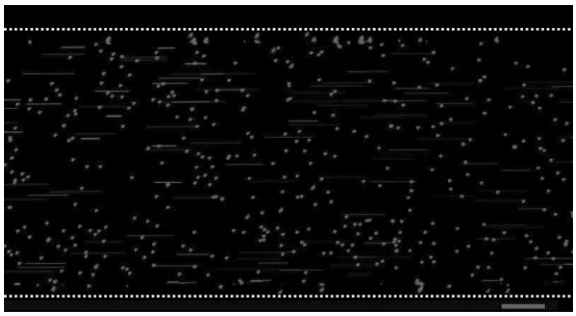

Fig. 3 Streaklines from 1 μm fluorescent microspheres at a flow rate of Q = 1.2 mL h^{-1} from a syringe pump. Measured maximum velocity in the microchannels was u_{max} = 2.38 mm s^{-1} compared to the theoretical prediction of u_{max} = 2.24 mm s^{-1}. Scale bar = 100 μm.

Statistical analysis

In total, three experiments (n = 3) were conducted for each condition, *i.e.* three microdevices were tested for each combination of cell type and protein. Three-way analysis of variance (ANOVA) was performed using Prostat 3.01 (Poly Software International, Inc., Pearl River, NY, USA) to analyze the effects of cell type (PAVECs or PAECs), protein type (FN or Col-I), protein coating concentration (500, 200, 100, 50, 10, or 0 μg mL^{-1}), or any interaction between the three factors for both cell spreading area and cell adhesion strength. Since no significant three-way interaction was found for either spreading area or adhesion strength, two-way ANOVAs were performed for each combination of two factors (collapsing over the third factor) to elucidate the main effects of each factor separately. For example, two-way ANOVA was performed for protein type and protein coating concentration for all PAEC data first, then for all PAVEC data (*i.e.* collapsing over cell types). If statistical significance was found between protein types, it was deemed a *main effect* of protein types averaged over all protein concentrations.

Simple effects were also analyzed using one-way ANOVAs for each factor at all different combinations of the remaining two factors. For example, for the combination of PAVECs on FN, one-way ANOVA was performed for all coating concentrations. Statistical significance in this case was then considered a *simple effect* in concentration, but only for PAVECs on FN. When necessary, multiple comparisons were performed using Tukey's method. Data was considered statistically significant only if $P < 0.01$.

Results

Cell spreading area

We first compared the ability of valvular endothelial cells (PAVECs) and vascular endothelial cells (PAECs) to spread and adhere to different ECM proteins over a range of protein concentrations. In general, PAECs spread well on both FN and Col-I, covering large regions of the microchannel surface

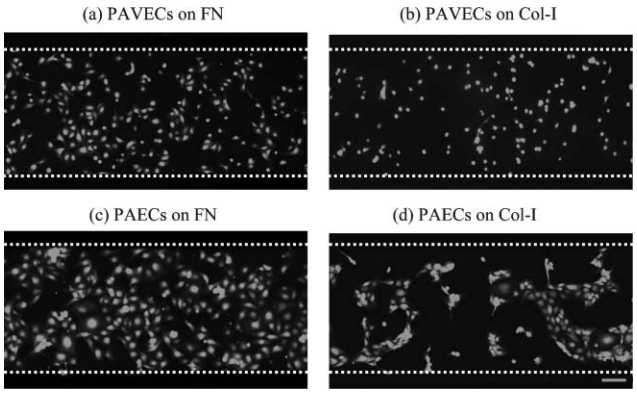

Fig. 4 Representative fluorescent images of cells on different protein coatings after two hour incubation. (a) PAVECs on FN coated at 500 μg mL^{-1}; (b) PAVECs on Col-I coated at 500 μg mL^{-1}; (c) PAECs on FN coated at 500 μg mL^{-1}; and (d) PAECs on Col-I coated at 500 μg mL^{-1}. Scale bar = 100 μm.

and forming visible networks with neighboring cells. In contrast, PAVECs spread well on FN, but not on Col-I (Fig. 4). Interestingly, PAVECs tended to be uniformly dispersed throughout the microchannel, and spread as individual cells without networking with their neighbors (see Fig. 4a,b), while PAECs maintained contact with adjacent cells, forming networked islands in confined regions of the microchannel (see Fig. 4c,d).

Morphological analyses confirmed that there was significant difference in cell spreading for PAVECs on FN *versus* Col-I (main effect, $P < 0.0001$), especially for 500, 200, and 100 μg mL^{-1} where FN resulted in larger cell areas (Fig. 5). Even at the highest Col-I concentration, PAVECs did not spread much more than on the control condition with no protein coating (240 ± 21 μm^2 *vs.* 199 ± 29 μm^2, respectively). For PAECs, a significant difference also existed between FN and Col-I (main effect, $P < 0.005$), but a simple effect was observed only for 500 μg mL^{-1} FN, which led to modestly larger cell areas (Fig. 5). By segregating the data based on protein type, comparisons were also made between cell types. For the FN coatings, no significant difference was found in

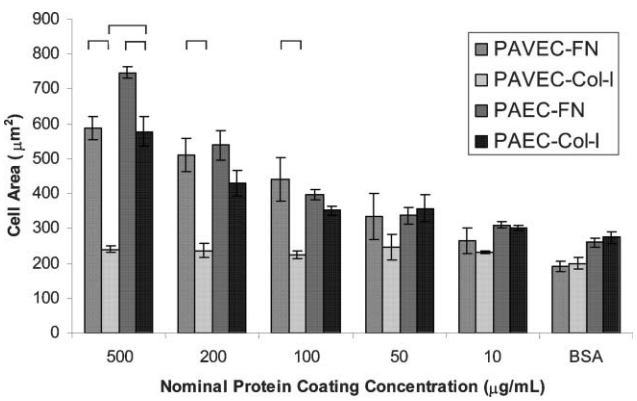

Fig. 5 Cell spreading area (μm^2) for cell–protein combinations at various levels of protein coating concentration. Data presented as mean ± SE ($n = 3$). Brackets indicate statistical significance, $P < 0.01$ (For clarity, some significant comparisons have not been shown).

spreading area between PAVECs and PAECs ($P > 0.05$). In contrast, for Col-I, there was a significant difference in spreading area between the cell types ($P < 0.0001$), with PAECs spreading much more than PAVECs. Thus, the level of spreading was cell-type dependent on Col-I, but not on FN.

Cell adhesion strength

Using the microfluidic device, we measured adhesion strength time profiles for all four cell–protein combinations at six levels of protein coating concentration (Fig. 6). Qualitative evaluation of these profiles shows that PAVECs were strongly attached to FN at 500 and 200 μg mL^{-1}, with almost 100% of all cells remaining after the entire shear assay (Fig. 6a). Likewise, PAVECs were moderately well attached at 100 μg mL^{-1} FN, with ~60% of the original number of cells remaining after the assay. In contrast, PAVECs were poorly attached to Col-I at all coating concentrations (Fig. 6b), with no significant difference in adhesion strength between concentrations ($P > 0.5$). For PAECs, excellent adhesion strength was observed for 500 μg mL^{-1} FN (Fig. 6c), while only moderate strength was observed for Col-I, even at 500 μg mL^{-1} (Fig. 6d). Equally poor adhesion strength was found for PAECs at all other concentrations for both protein types.

The dynamics of cell detachment were further investigated to confirm that cells detached abruptly at a given shear level and were not simply slowly peeling off as the shear stress was increased with each step. We observed that for each steady shear stress level in the stepped approach, the number of attached cells always decreased quickly in the first 30 s to a steady value (see ESI‡). The number of attached cells then remained constant for the remaining 3.5 min of each interval, until the next shear stress level was applied. In addition, when 220 dyn cm^{-2} was constantly applied for 12 min, the number of attached cells decreased abruptly to a steady value within the first 90 s, and then remained constant for the remaining 10.5 min (see the ESI‡). Moreover, this steady value matched that from the ramped shear experiment after exposure to 220 dyn cm^{-2}. This confirmed that cells did not gradually detach over time, but instead responded quickly to shear at each level.

Fig. 7 shows the average adhesion strength parameter (ASP, defined in the methods section) for each cell–protein condition. For all FN coatings, PAVECs were more strongly attached than PAECs (main effect, $P < 0.0005$); however, no significant difference between cell types was found for Col-I data ($P > 0.05$). When data were segregated by cell type, significant difference was found between FN and Col-I only for PAVECs on 500 μg mL^{-1} ($P < 0.01$); data was not significant at all other protein concentrations for both cell types.

Discussion

It has been previously shown that vascular and valvular endothelial cells exhibit distinct morphologies and develop unique reorganization of focal adhesion complexes under dynamic shear conditions.[8] When grown to confluence on Col-I and exposed to long-term shear stress at approximately physiological levels, aortic endothelial cells elongated and aligned parallel to the flow direction, and focal adhesion

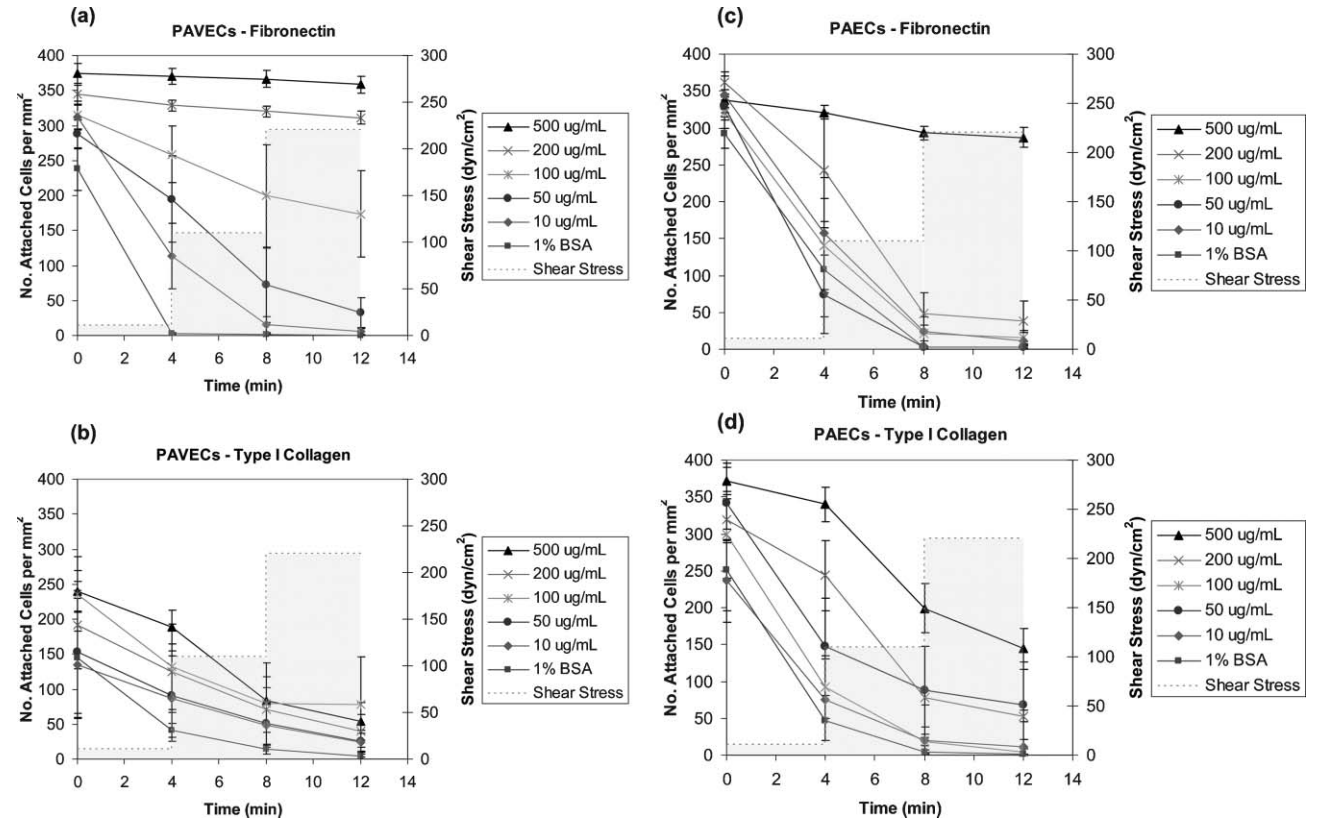

Fig. 6 Adhesion strength time profiles. Number of attached cells per mm^2 of microchannel surface is plotted *versus* time exposed to shear (left axis). Dotted line represents shear stress level applied, 4 min at 11 dyn cm^{-2}, 4 min at 110 dyn cm^{-2} and 4 min at 220 dyn cm^{-2} (all nominal design values) (right axis). (a) PAVECs on FN; high adhesion strength for 500, 200, and 100 μg mL^{-1}. (b) PAVECs on Col-I; poor adhesion strength for all concentrations. (c) PAECs on FN; high adhesion strength for 500 μg mL^{-1} only. (d) PAECs on Col-I; moderate adhesion strength for 500 μg mL^{-1} only. Data presented as mean ± SE (n = 3).

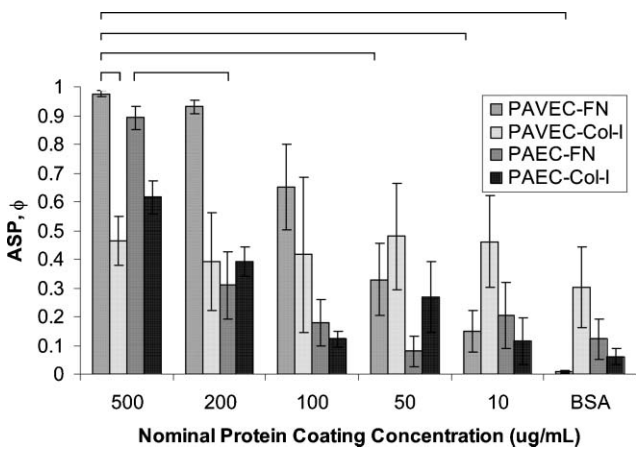

Fig. 7 Adhesion strength parameter, ϕ, for different cell–protein combinations at various levels of protein coating concentration. Data presented as mean ± SE (n = 3). Brackets indicate statistical significance, $P < 0.01$ (For clarity, some significant comparisons have not been shown).

components were found to cluster at the tips of the major axis upstream and downstream of flow. In contrast, aortic valve endothelial cells elongated and aligned perpendicular to the flow direction, and while focal adhesion components also clustered at the tips of the major axis, these locations coincided with a perpendicular polarization neither upstream nor downstream of flow. These observations provided preliminary evidence that the two closely-related and neighboring cell types are in fact phenotypically different.

In the current study, we report for the first time, quantitative comparisons between the interaction of vascular and valvular endothelial cells with their matrix. These data provide novel evidence in support of phenotypic heterogeneity between vascular and valvular endothelial cell populations.[25] While PAECs were well spread on both FN and Col-I, PAVECs were only well spread on FN and not at all on Col-I. And while PAECs adhered strongly to high concentrations of both FN and Col-I, PAVECs adhered strongly only to FN at moderate to high concentrations, but not at all on Col-I. From these observations, it is evident that the extent of spread and the strength of attachment depend not only on the type of ECM protein, but also on the cell type.

It is likely that the dissimilarities in adhesion properties between the two cell types reflect differences in integrin expression, activation, and distribution. Integrin expression in healthy human hearts is distinct between the aorta and the aortic valve.[26] Notably, the integrin receptor for Col-I (α2β1) is expressed in the aorta, but not the aortic valve, whereas the integrin that binds FN (α5β1) is equally expressed in the two tissues. This expression pattern *in vivo* is consistent with our current observations that PAVECs attach only to FN *in vitro*,

whereas PAECs are able to bind to both FN and Col-I. These observations not only provide new evidence that PAVECs and PAECs are phenotypically different, but also suggest that the matrix protein may differentially modulate the biological responses of vascular *versus* valvular endothelial cells when exposed to long-term shear stress. Shear stress regulates a number of important endothelial responses that are mediated through pathways involving integrins and the extracellular matrix components to which they are attached. The availability of different matrix components for attachment can therefore alter the response of a particular cell type.[7,27] This has implications for the selection of matrix proteins in endothelialized microdevices and engineered tissues. It may also explain the differences observed between vascular and valvular endothelial cells in response to shear when grown on Col-I.[8]

The current results should be interpreted with due consideration of the physical environment within which the cells were cultured. The microfluidic environment presents a vastly different cell culture milieu compared to conventional culturing platforms, such as Petri dishes and flasks.[28] One of the most important microscale-dominant phenomena is diffusion.[28,29] In our experiments, during the two hour incubation when cells spread and attach, the cells were in a static microenvironment where soluble factors travelled to neighboring cells by diffusion alone. This is in contrast to conventional macroscale cell culture where convective transport plays a greater role. Because of the high cell surface density achieved in the present experiments, the local accumulation of biological factors was likely much higher than what would occur at the macroscale, even for a shorter time of culture. The effects of higher concentrations of soluble factors produced by endothelial cells during microscale culture, particularly in promoting or inhibiting the spreading and attachment of nearby cells through paracrine and autocrine signaling, is largely unknown. Research in this area would benefit our understanding of microscale cellular studies, and potentially improve current methods for culturing cells in the microenvironment.

Our procedure for coating the microchannels with proteins was rapid and required less reagent volume than previous methods.[21] Using indirect immunostaining with anti-FN and anti-Col-I antibodies and measuring fluorescence intensity, we confirmed that higher inoculated protein concentrations indeed led to higher levels of protein adsorption to the glass substrate (data not shown). Since PDMS is hydrophobic and permissive to protein adsorption, we also observed some adsorption to the side walls. Although adsorption of proteins from the culture medium was also a consideration because of the high surface-to-volume ratio at the microscale,[28] this effect was likely minor because we blocked with BSA after protein coating. Considering the simplicity and effectiveness of our protein loading and coating procedure, it may find widespread utility in many other microfluidic cell culture studies. Further, as demonstrated here, the use of parallel networks of microchannels provides a simple method to rapidly determine the optimal protein type and coating density required for cell adhesion, which will be useful for both conventional and microfluidic cell culture.

Understanding cell adhesion at the microscale allows us to extend current methods to long-term culture for fundamental studies of endothelial cell biology. Furthermore, the current results apply not only to cell culture, but also to the endothelialization of biomaterials for the regeneration of tissues, such as heart valves.[30] While some researchers have specifically examined *valve* endothelial cell growth and morphology on different biomaterials,[31,32] the majority of efforts to engineer heart valves have used *vascular* endothelial cells.[20,33,34] It has been suggested that failures of current tissue engineered heart valves stem in part from the use of vascular endothelial cells, instead of more regionally-compatible valve endothelial cells.[12] Our data provide new evidence of phenotypic and functional heterogeneity in endothelial cells and suggest that the adhesion and function of endothelial cells on tissue engineered valves (and consequently the success of the valves) is strongly dependent on the type of cell used and the nature of the biomaterial substrate.

Conclusion

Vascular and valvular endothelial cells exhibited unique cell spreading and adhesion strength on different extracellular matrix proteins in microfluidic channels. Valve endothelial cells preferentially adhered to fibronectin, displaying both improved spreading and attachment strength compared to type I collagen at any concentration. In contrast, vascular endothelial cells adhered relatively well to both matrix proteins, with slightly stronger adherence to fibronectin. Overall, fibronectin was demonstrated to be the protein of choice for enhancing spreading and adhesion strength of endothelial cells in microchannels. More importantly, cell adhesion properties were cell-type and matrix dependent. This suggests that experiments involving mechanobiological responses of endothelial cells to shear stress must take into account the type of matrix protein for a given cell type. All of these findings were facilitated by the design and fabrication of a parallel network of microchannels, which permitted simultaneous evaluation of different conditions in a cellular microenvironment suitable for studying cell biology and with application to tissue engineering.

Acknowledgements

We thank Mohamed Abdelgawad, Lindsey Fiddes, Yali Gao, and Chris Moraes for helpful discussions on microfabrication. We thank Prof. Axel Günther and Prof. William Stanford for use of their facilities, and Dan Trcka from the Langille Lab for providing aortic endothelial cells. We acknowledge financial support from the Glynn Williams Fellowship to EY, the Canada Foundation for Innovation, the Canada Research Chair in Mechanobiology to CAS, and the Canada Research Chair in Bioanalytical Chemistry to ARW.

References

1 R. Ross, The Pathogenesis of Atherosclerosis—a Perspective for the 1990s, *Nature*, 1993, **362**, 801–809.
2 M. Thubrikar, *The Aortic Valve*, CRC Press, Inc., Boca Raton, Florida, 1990, pp. 21–33.

3 B. Alberts, A. Johnson, J. Lewis, M. Raff, K. Roberts and P. Walter, *Molecular Biology of the Cell*, Garland Science, New York, 2002, pp. 1090–1109.
4 R. O. Hynes, Integrins: Versatility, Modulation, and Signaling in Cell-Adhesion, *Cell*, 1992, **69**, 11–25.
5 R. L. Juliano and S. Haskill, Signal Transduction from the Extracellular Matrix, *J. Cell Biol.*, 1993, **120**, 577–585.
6 P. F. Davies, Flow-Mediated Endothelial Mechanotransduction, *Physiol. Rev.*, 1995, **75**, 519–560.
7 A. W. Orr, J. M. Sanders, M. Bevard, E. Coleman, I. J. Sarembock and M. A. Schwartz, The Subendothelial Extracellular Matrix Modulates Nf-Kappa B Activation by Flow: A Potential Role in Atherosclerosis, *J. Cell Biol.*, 2005, **169**, 191–202.
8 J. T. Butcher, A. M. Penrod, A. J. Garcia and R. M. Nerem, Unique Morphology and Focal Adhesion Development of Valvular Endothelial Cells in Static and Fluid Flow Environments, *Arterioscler., Thromb., Vasc. Biol.*, 2004, **24**, 1429–1434.
9 S. Noria, D. B. Cowan, A. I. Gotlieb and B. L. Langille, Transient and Steady-State Effects of Shear Stress on Endothelial Cell Adherens Junctions, *Circ. Res.*, 1999, **85**, 504–514.
10 M. J. Levesque and R. M. Nerem, The Elongation and Orientation of Cultured Endothelial Cells in Response to Shear Stress, *J. Biomech. Eng.*, 1985, **107**, 341–347.
11 B. R. Blackman, K. A. Barbee and L. E. Thibault, In Vitro Cell Shearing Device to Investigate the Dynamic Response of Cells in a Controlled Hydrodynamic Environment, *Ann. Biomed. Eng.*, 2000, **28**, 363–372.
12 J. T. Butcher and R. M. Nerem, Valvular Endothelial Cells Regulate the Phenotype of Interstitial Cells in Co-Culture: Effects of Steady Shear Stress, *Tissue Eng.*, 2006, **12**, 905–915.
13 B. L. Gray, D. K. Lieu, S. D. Collins, R. L. Smith and A. I. Barakat, Microchannel Platform for the Study of Endothelial Cell Shape and Function, *Biomed. Microdev.*, 2002, **4**, 9–16.
14 J. W. Song, W. Gu, N. Futai, K. A. Warner, J. E. Nor and S. Takayama, Computer-Controlled Microcirculatory Support System for Endothelial Cell Culture and Shearing, *Anal. Chem.*, 2005, **77**, 3993–3999.
15 C. Fidkowski, M. R. Kaazempur-Mofrad, J. Borenstein, J. P. Vacanti, R. Langer and Y. D. Wang, Endothelialized Microvasculature Based on a Biodegradable Elastomer, *Tissue Eng.*, 2005, **11**, 302–309.
16 A. Paguirigan and D. J. Beebe, Gelatin Based Microfluidic Devices for Cell Culture, *Lab Chip*, 2006, **6**, 407–413.
17 S. W. Rhee, A. M. Taylor, C. H. Tu, D. H. Cribbs, C. W. Cotman and N. L. Jeon, Patterned Cell Culture inside Microfluidic Devices, *Lab Chip*, 2005, **5**, 102–107.
18 W. Tan and T. A. Desai, Microscale Multilayer Cocultures for Biomimetic Blood Vessels, *J. Biomed. Mater. Res., Part A*, 2005, **72A**, 146–160.
19 A. P. McGuigan and M. V. Sefton, Vascularized Organoid Engineered by Modular Assembly Enables Blood Perfusion, *Proc. Natl. Acad. Sci. U. S. A.*, 2006, **103**, 11461–11466.
20 S. P. Hoerstrup, R. Sodian, S. Daebritz, J. Wang, E. A. Bacha, D. P. Martin, A. M. Moran, K. J. Guleserian, J. S. Sperling, S. Kaushal, J. P. Vacanti, F. J. Schoen and J. E. Mayer, Functional Living Trileaflet Heart Valves Grown in Vitro, *Circulation*, 2000, **102**, 44–49.
21 H. Lu, L. Y. Koo, W. M. Wang, D. A. Lauffenburger, L. G. Griffith and K. F. Jensen, Microfluidic Shear Devices for Quantitative Analysis of Cell Adhesion, *Anal. Chem.*, 2004, **76**, 5257–5264.
22 D. C. Duffy, J. C. McDonald, O. J. A. Schueller and G. M. Whitesides, Rapid Prototyping of Microfluidic Systems in Poly(Dimethylsiloxane), *Anal. Chem.*, 1998, **70**, 4974–4984.
23 R. K. Shah and A. L. London, *Laminar Flow Forced Convection in Ducts*, Academic Press, New York, 1978, pp. 196–202.
24 D. Sinton, Microscale Flow Visualization, *Microfluid. Nanofluid.*, 2004, **1**, 2–21.
25 P. F. Davies, A. G. Passerini and C. A. Simmons, Aortic Valve - Turning over a New Leaf(Let) in Endothelial Phenotypic Heterogeneity, *Arterioscler., Thromb., Vasc. Biol.*, 2004, **24**, 1331–1333.
26 M. Wilhelmi, S. Fischer, R. Leyh, H. Mertsching and A. Haverich, Endothelial Anatomy of the Human Heart: Immunohistochemical Evaluation of Endothelial Differentiation, *Thorac. Cardiov. Surg.*, 2002, **50**, 230–236.
27 A. W. Orr, B. P. Helmke, B. R. Blackman and M. A. Schwartz, Mechanisms of Mechanotransduction, *Dev. Cell*, 2006, **10**, 11–20.
28 G. M. Walker, H. C. Zeringue and D. J. Beebe, Microenvironment Design Considerations for Cellular Scale Studies, *Lab Chip*, 2004, **4**, 91–97.
29 H. M. Yu, I. Meyvantsson, I. A. Shkel and D. J. Beebe, Diffusion Dependent Cell Behavior in Microenvironments, *Lab Chip*, 2005, **5**, 1089–1095.
30 I. Vesely, Heart Valve Tissue Engineering, *Circ. Res.*, 2005, **97**, 743–755.
31 J. L. Cuy, B. L. Beckstead, C. D. Brown, A. S. Hoffman and C. M. Giachelli, Adhesive Protein Interactions with Chitosan: Consequences for Valve Endothelial Cell Growth on Tissue-Engineering Materials, *J. Biomed. Mater. Res., Part A*, 2003, **67A**, 538–547.
32 S. Brody, J. McMahon, L. Yao, M. O'Brien, P. Dockery and A. Pandit, The Effect of Cholecyst-Derived Extracellular Matrix on the Phenotypic Behaviour of Valvular Endothelial and Valvular Interstitial Cells, *Biomaterials*, 2007, **28**, 1461–1469.
33 G. Steinhoff, U. Stock, N. Karim, H. Mertsching, A. Timke, R. R. Meliss, K. Pethig, A. Haverich and A. Bader, Tissue Engineering of Pulmonary Heart Valves on Allogenic Acellular Matrix Conduits - in Vivo Restoration of Valve Tissue, *Circulation*, 2000, **102**, 50–55.
34 R. G. Leyh, M. Wilhelmi, T. Walles, K. Kallenbach, P. Rebe, A. Oberbeck, T. Herden, A. Haverich and H. Mertsching, Acellularized Porcine Heart Valve Scaffolds for Heart Valve Tissue Engineering and the Risk of Cross-Species Transmission of Porcine Endogenous Retrovirus, *J. Thorac. Cardiovasc. Surg.*, 2003, **126**, 1000–1004.

